UNIVERSITY OF
BATH

Citation for published version:
Wang, YY, Peng, X, Alharbi, M, Dutin, CF, Bradley, TD, Gérôme, F, Mielke, M, Booth, T & Benabid, F 2012, 'Design and fabrication of hollow-core photonic crystal fibers for high-power ultrashort pulse transportation and pulse compression', Optics Letters, vol. 37, no. 15, pp. 3111-3113. https://doi.org/10.1364/OL.37.003111

DOI:
10.1364/OL.37.003111

Publication date:
2012

Document Version
Publisher's PDF, also known as Version of record

Link to publication

University of Bath

Design and fabrication of hollow-core photonic crystal fibers for high-power ultrashort pulse transportation and pulse compression

Y. Y. Wang,[1,2] Xiang Peng,[3] M. Alharbi,[1,2] C. Fourcade Dutin,[1] T. D. Bradley,[1,2] F. Gérôme,[2] Michael Mielke,[3] Timothy Booth,[3] and F. Benabid[1,2,*]

[1]*Gas-Phase Photonic Material Group, CPPM, Physics Department, University of Bath, UK*

[2]*GPPMM Group, Xlim Research Institute, CNRS UMR 7252, University of Limoges, France*

[3]*Raydiance Inc., 2199 S. McDowell Boulevard, Suite 140, Petaluma, California 94547, USA*

*Corresponding author: f.benabid@xlim.fr

We report on the recent design and fabrication of kagome-type hollow-core photonic crystal fibers for the purpose of high-power ultrashort pulse transportation. The fabricated seven-cell three-ring hypocycloid-shaped large core fiber exhibits an up-to-date lowest attenuation (among all kagome fibers) of 40 dB/km over a broadband transmission centered at 1500 nm. We show that the large core size, low attenuation, broadband transmission, single-mode guidance, and low dispersion make it an ideal host for high-power laser beam transportation. By filling the fiber with helium gas, a 74 µJ, 850 fs, and 40 kHz repetition rate ultrashort pulse at 1550 nm has been faithfully delivered at the fiber output with little propagation pulse distortion. Compression of a 105 µJ laser pulse from 850 fs down to 300 fs has been achieved by operating the fiber in ambient air.   © 2012 Optical Society of America

OCIS codes: 060.3510, 060.5295, 140.3510.

The recent advances in high-power ultrashort pulsed lasers (pulse width <1 ps) and their wide use in applications as varied as biophotonics, micromachining, surface marking, texturing, sensing, and military applications [1–3] call for a flexible and robust means for beam delivery over a several meter-long optical path. An "ideal" transport solution for such ultrashort pulses (USPs) requires low propagation loss and low dispersion, high input coupling efficiency, high damage threshold, and single-mode guidance over a large optical bandwidth. Unfortunately, silica-core-based optical fiber is only capable of nanojoule pulse energy in the USP regime [4] due to its low material damage threshold, high dispersion, and other nonlinear effects. More recently, photonic bandgap (PBG) hollow-core photonic crystal fiber (HC-PCF) was used for power delivery [5,6]. However, the fiber has a limited bandwidth (∼70 THz) and a small core size (∼10 µm). Also, its guided core mode suffers from a large spatial overlap with the silica core wall, thus limiting the coupled power level to be within several microjoules.

In parallel, work on kagome lattice cladding HC-PCF shows that this type of fiber exhibits broadband guidance, low spatial overlap with silica, and low group velocity dispersion [7]. These attributes make such a fiber a good candidate for many applications [8], including USP delivery [9,10]. Indeed, microjoule level USP has already been delivered using a kagome fiber [9]. However, the maximum energy demonstrated was limited to 10 µJ at 800 nm [9]. Recently, a hypocycloid-core kagome HC-PCF was demonstrated [11] showing attenuation figure as low as 180 dB/km at near IR over optical transmission bandwidth of 200 THz, and lower optical power overlap with the core silica surround.

Here we report, for the first time to our knowledge [12], a hypocycloid-shaped large core (∼70 µm) kagome-type HC-PCF with a record loss figure of 40 dB/km over a broadband transmission from 1100 to >1750 nm [limit

of the optical spectral analyzer (OSA)]. Furthermore, the fiber exhibits single-mode operation. By filling this fiber with helium gas to minimize optical nonlinearities and compensate the small waveguide dispersion, we demonstrate delivery at the fiber output of 74 µJ, 850 fs, and 40 kHz repetition rate USP (peak power 87 MW, average power 3 W) operating around 1550 nm. With air-filled HC-PCF, we demonstrate a compression of 850 fs wide and 105 µJ energy USP down to 300 fs. To the best of our knowledge, this is the first demonstration of an optical device that combines high power handling, ultra-low pulse temporal spreading, and pulse compression capabilities for high-power USP.

Figure 1(a) shows the scanning electronic micrograph of the seven-cell three-ring hypocycloid-core kagome fiber we fabricated. The hypocycloid core is created by removing the seven central capillaries and carefully controlling the relative pressures between the core and the cladding during the fiber drawing [11]. The fiber presents an outer diameter of 300 µm, a pitch of 23 µm, and a strut thickness of 350 nm. The hypocycloid core exhibits a subjacent inner circle with a diameter of ∼66 µm and an outer circle with a diameter of 79 µm [Fig. 1(b)], introducing no distortion to the first cladding ring.
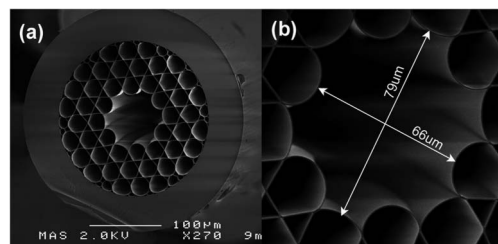

Fig. 1.   Scanning electronic micrograph (SEM) of the fabricated seven-cell three-ring hypocycloid-core kagome fiber showing (a) the whole structure and (b) the 66–79 µm core.

Figure 2(b) shows the optical attenuation spectrum of this fiber obtained by a cutback measurement using both a white light lamp source and a supercontinuum source from a 55 m length fiber to a 5 m length fiber [Fig. 2(a)]. It shows a record baseline of 40 dB/km (± 5 dB/km) over a bandwidth spanning from 1100 to >1750 nm (limit of OSA) and reaching a minimum of 33 dB/km at 1440 nm and 1490 nm. This beats the PBG HC-PCF in terms of bandwidth (~ 70 THz for PBG) and demonstrates a comparable loss figure [13]. Compared to the fiber we previously reported in [11], the larger core size increases the laser-induced damage threshold and the 4 times smaller propagation loss means less scattering and radiation to the silica cladding. Figure 2(b) also shows the calculated group velocity dispersion (GVD), which shows an anomalous dispersion over most of the transmission windows with a value of ~ 2 ps/nm/km around the wavelength range of interest 1500–1600 nm.

Despite the relatively large core size of the fiber, and provided a good NA matching (NA ~ 0.023), the fiber guides light in a single-mode fashion and the coupling efficiency exceeds 90%. Figures 2(c)–2(f) show the mode profiles of the fiber. Both the calculated and measured mode field diameter (MFD) shows a value of $\sim 47\ \mu$m [Figs. 2(c) and 2(e)], much smaller than the core size (66–79 μm). This MFD approaches that of a capillary with a bore diameter equal to the inner diameter of the hypocycloid core of the HC-PCF. This implies a reduction of the spatial overlap of the core mode with the silica core wall, making it thus a good candidate for beam delivery.

To test the fiber's capability in transporting high-power USP with no pulse spreading on one hand and in pulse compression on the other hand, we launch the output beam of a USP laser operating at 1550 nm with pulse width in the range of 0.9 and 0.8 ps, a pulse energy of 105 μJ, and a repetition rate of 40 kHz into ~ 2.3 m long HC-PCF. Figure 3 shows the setup for the pulse-spread free

experiment. By matching the NA of the incoming beam to that of the fiber, a coupling efficiency of >90% has been achieved. Note that the maximum coupling is done at very low pulse energy ($\sim 0.5\ \mu$J) so to avoid damage to the silica struts of the fiber. After that, the launched energy is slowly increased to minimize thermal shock, which has been observed to cause slight fiber movements and hence fiber damage. This issue would be negated by rigid mounting of the fiber tip and a better thermal management design. The output of the kagome fiber is sealed in a chamber and 3.4 bar helium is introduced to the fiber through this chamber so to minimize the effect of nonlinearity in the hollow core [helium has a much smaller nonlinear refractive index ($n_2 \sim 4 \times 10^{-25}$ m^2/W) than most other noble gases (usually of the order of 10^{-23} m^2/W)] and also cooling the fiber end. At the output, a power meter, USP laser intensity autocorrelator (AC), OSA, and a scanning slit beam profiler (Nanoscan) are consecutively positioned to measure the beam characteristics.

Figures 4(a)–4(c) show the spectral and temporal trace of the delivered pulse with different energies. As a reference, the input pulse is first monitored, as shown in the gray dashed curve in Fig. 4(a) OSA trace and Fig. 4(b) AC trace. By rotating the half-wave plate at the input, different output pulse energies were obtained. Figure 4(a) shows the output spectrum for output energies varying from 10 to 74 μJ with different colored curves. One can see that there are no significant changes between these spectra. Similarly, in Fig. 4(b), the AC traces show negligible changes when the output energy varies from 30 to 70 μJ. The deduced temporal pulse width at FWHM for each AC trace is shown in Fig. 4(c). The pulses have a FWHM of 830, 837, 803, 854, and 844 fs, respectively, all similar to that of the input pulse (850 fs). These results show the shape of the pulse in both frequency domain and the time domain has been well maintained with insignificant optical nonlinearity and propagation linear dispersion. This is so, even when the input peak intensity exceeds 5 TW/cm^2. This also indicates the little optical power overlap with silica core surround. It is noteworthy that the highest output pulse energy of 74 μJ is limited by the maximum input laser pulse energy of $\sim 100\ \mu$J. The coupling efficiency here is not as high as 90% (obtained with low input energy) probably because of slightly coupling drift, or an onset of nonlinear effects, such as photoionization. However, with 74 μJ output pulse energy obtained, no damage to the fiber has been observed. This value is much higher than previously reported USP delivery using HC-PCF [6,9]. Furthermore,
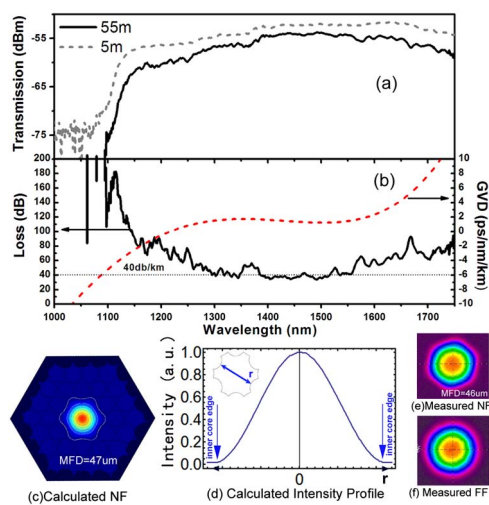
Fig. 2. (Color online) (a) Fiber optical transmission spectra. (b) The fiber optical attenuation spectrum (solid black curve) and calculated GVD (dashed red curve). The dotted horizontal curve shows the baseline of the attenuation figure. (c) Calculated near-field (NF) pattern with an MFD of 47 μm. (d) Calculated intensity profile showing along the axis shown in the top left insert. (e) Measured NF pattern showing. (f) Measured far-field (FF) pattern.
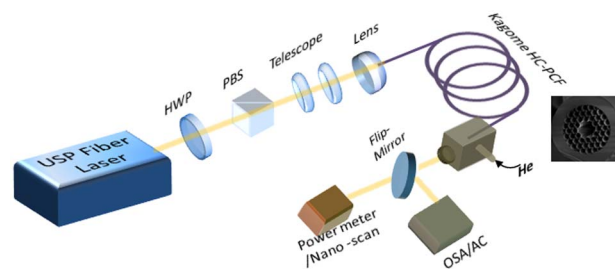
Fig. 3. (Color online) Setup of the pulse-spread free experiment. HWP, half-wave plate; PBS, polarizing beam splitter; OSA, optical spectrum analyzer; AC, second-harmonic intensity autocorrelator.
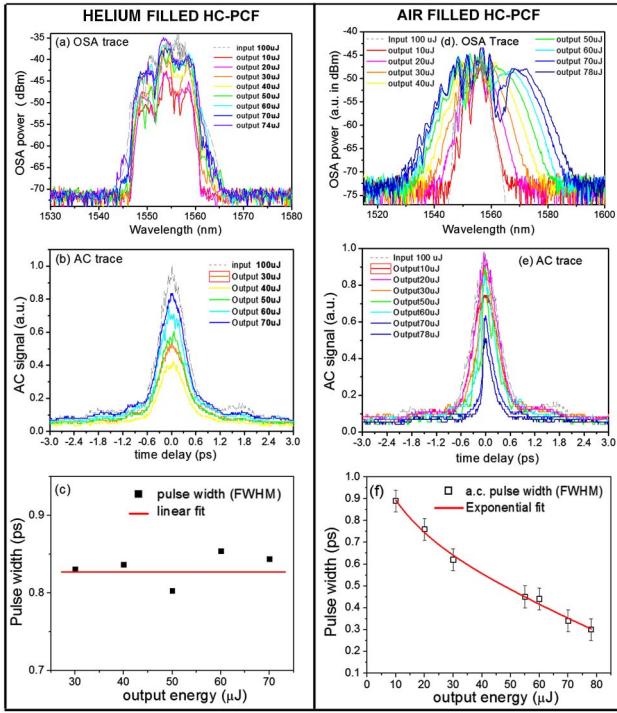
Fig. 4. (Color online) Left: pulse-spread free experiment when the fiber is filled with helium. (a) Fiber output optical spectra of the fiber for different output pulse energies and the laser spectrum at 100 μJ (gray dashed curve), (b) intensity autocorrelation (AC) traces, and (c) FWHM pulse durations versus output pulse energy (solid squares) and a linear fit (red line) for an HC-PCF filled with 3.4 bar of helium. Right: same with an HC-PCF filled with ambient air. In (f), the error bar is ± 0.05 ps due to AC resolution, and the fit curve is for visual guidance.

the 100 μJ pulse transported by the fiber corresponds to a fluence of 6 J/cm^2, which is 3 times larger than fused silica laser damage threshold with subpicosecond pulses. In order to have a qualitative estimate on the upper-limit of the energy that could be handled by the fiber, a similar kagome fiber tailored for a guidance around 1 μm was tested with 12 ns pulses from an Nd:YAG laser. Input pulses with energy as high as 10 mJ were transported with no damage to the fiber; corresponding to a fluence of 2000 J/cm^2, which is 40 times higher than the fused silica laser damage threshold. Consequently, one could project that transportation of millijoule energy-level subpicoseconds pulses is possible with this HC-PCF.

For the pulse compression experiment, the experimental protocol is similar to Fig. 3 except that the kagome fiber is exposed to the ambient air, which has n_2 of $\sim 4 \times 10^{-23}$ m^2/W. Figures 4(d)–4(f) summarize the results. The input pulse shape is shown in the gray dashed curve for both OSA trace and AC trace. With 10 μJ energy, the onset of spectral broadening is observed as shown in Fig. 4(d) red curve. By increasing the input energy, the broadening of the output spectra is much clearer, proportional to the input pulse energy, as shown in different colors in Fig. 4(d). The near-symmetrical broadening of the spectra is indicative of self-phase modulation being the dominant optical nonlinear mechanism [14]. This is corroborated with the temporal pulse traces

shown in Fig. 4(e). Pulse compression down to ~ 300 fs has been observed [Fig. 4(e) purple curve] when the input pulse energy is on the maximum of 105 μJ and the output pulse energy is 78 μJ. It is noteworthy that the compression was achieved directly from the fiber output as one would expect from an anomalous dispersive media [14]. This means a peak power of 240 MW and peak intensity exceeding 10 TW/cm^2, which is more than twice that of the original pulse. The evolution of the pulse duration versus pulse energy is plotted in Fig. 4(f). The pulse duration decreases in an exponential decay manner with the increase of the pulse energy.

In conclusion, we fabricated a seven-cell three-ring hypocycloid-core kagome HC-PCF with a record optical attenuation of 40 dB/km over a large spectral window with single-mode guidance and relatively low bending loss. The fiber proved to be an excellent means for high-power USP beam delivery with no pulse temporal broadening nor damage and for pulse compression. We believe by using a more powerful laser, delivery and compression of a pulse with more energy is possible. In the future, by further increasing the fiber's hollow-core size, the laser-induced damage threshold should be further increased and could potentially meet the beam delivery requirements of the increasingly powerful short-pulse lasers.

References

1. B. N. Chichkov, C. Momma, S. Nolte, F. von Alvensleben, and A. Tünnermann, Appl. Phys. A **63**, 109 (1996).
2. M. Mielke, D. Gaudiosi, K. Kim, M. Greenberg, X. Gu, R. Cline, X. Peng, M. Slovick, N. Allen, M. Manning, M. Ferrel, N. Prachayaamorn, and S. Sapers, J. Laser. Micro/Nanoeng. **5**, 53 (2010).
3. H. Loesel, J. P. Fischer, M. H. Götz, C. Horvath, T. Juhasz, F. Noack, N. Suhm, and J. F. Bille, Appl. Phys. B **66**, 121 (1998).
4. A. V. Smith, B. T. Do, G. R. Hadley, and R. L. Farrow, IEEE J. Sel. Top. Quantum Electron. **15**, 153 (2009).
5. F. Luan, J. Knight, P. Russell, S. Campbell, D. Xiao, D. Reid, B. Mangan, D. Williams, and P. Roberts, Opt. Express **12**, 835 (2004).
6. X. Peng, M. Mielke, and T. Booth, Opt. Express **19**, 923 (2011).
7. F. Couny, F. Benabid, P. J. Roberts, P. S. Light, and M. G. Raymer, Science **318**, 1118 (2007).
8. F. Benabid, Phil. Trans. R. Soc. A **364**, 3439 (2006).
9. O. H. Heckl, C. R. E. Baer, C. Kränkel, S. V. Marchese, F. Schapper, M. Holler, T. Südmeyer, J. S. Robinson, J. W. G. Tisch, F. Couny, P. Light, F. Benabid, and U. Keller, Appl. Phys. B **97**, 369 (2009).
10. O. H. Heckl, C. J. Saraceno, C. R. E. Baer, T. Südmeyer, Y. Y. Wang, Y. Cheng, F. Benabid, and U. Keller, Opt. Express **19**, 19142 (2011).
11. Y. Y. Wang, N. V. Wheeler, F. Couny, P. J. Roberts, and F. Benabid, Opt. Lett. **36**, 669 (2011).
12. Y. Y. Wang, X. Peng, M. Alharbi, C. Fourcade Dutin, T. D. Bradley, F. Gérôme, M. Mielke, T. Booth, and F. Benabid, Proc. SPIE **8269**, 826907 (2012).
13. P. J. Roberts, F. Couny, H. Sabert, B. J. Mangan, D. P. Williams, L. Farr, M. W. Mason, A. Tomlinson, T. A. Birks, J. C. Knight, and P. St. J. Russell, Opt. Express **13**, 236 (2005).
14. D. Anderson, M. Desaix, M. Lisak, and M. L. Quiroga-Teixeiro, J. Opt. Soc. Am. B **9**, 1358 (1992).